Writing of nonlinear optical $Sm_2(MoO_4)_3$ crystal lines at the surface of glass by samarium atom heat processing

M. Abe, Y. Benino, T. Fujiwara, and T. Komatsu[a)]
Department of Chemistry, Nagaoka University of Technology, 1603-1 Kamitomioka-cho, Nagaoka 940-2188, Japan

R. Sato
Department of Materials Engineering, Tsuruoka National College of Technology, Tsuruoka 997-8511, Japan

(Received 16 February 2005; accepted 25 April 2005; published online 20 June 2005)

Some glasses such as $21.25Sm_2O_3.63.75MoO_3.15B_2O_3$ (mol %) giving the formation of nonlinear optical $Sm_2(MoO_4)_3$ crystals through conventional crystallization in an electric furnace and through continuous-wave Nd: yttrium aluminum garnet (YAG) laser (wavelength: 1064 nm) irradiation (*samarium atom heat processing*) have been developed. It is proposed from x-ray diffraction analyses, micro-Raman-scattering spectra, and second-harmonic generation measurements that the crystal structure of $Sm_2(MoO_4)_3$ formed by the crystallization is the β'-phase structure with an orthorhombic (noncentrosymmetric) symmetry. The lines consisting of nonlinear optical β' -$Sm_2(MoO_4)_3$ crystals are written at the surface of glasses by YAG laser irradiation (laser power: $P=0.4$ W, laser scanning speed: $S=1-10$ μm/s), and, in particular, homogeneous crystal lines are formed at the laser scanning speed of 1 μm/s. Refractive index changes (not crystallization) are also induced by YAG laser irradiation of $P=0.4$ W and a high laser scanning speed of $S=25$ μm/s. The crystallization mechanism in the laser-irradiated region has been proposed. The present study demonstrates that the samarium atom heat processing is a technique for the writing of rare earth containing optical nonlinear/ferroelectric crystal lines in glass. © *2005 American Institute of Physics*. [DOI: 10.1063/1.1938269]

I. INTRODUCTION

Crystallization of glass is a method for fabrication of transparent and dense condensed materials with desired shapes and also nanostructures.[1–4] Usually, crystallized glasses (glass ceramics) are fabricated using well-controlled heat treatment in an electric furnace, and desired crystals are formed at the surface or in the interior of glass. Laser irradiation of glass has been regarded as a process for spatially selected structural modification and crystallization in glass, and recently, various studies in laser-induced structural changes have been carried out so far, where the most of target glasses are SiO_2-based glasses, source lasers are mainly short-wavelength excimer lasers or femtosecond pulsed lasers, and structural modifications are refractive index changes (not crystallization).[5–9]

The present authors' group[10–18] proposed that the irradiation of a continuous-wave (cw) Nd: yttrium aluminum garnet (YAG) laser with a wavelength of $\lambda=1064$ nm induces the formation of crystal dots and lines such as $Sm_xBi_{1-x}BO_3$, β -BaB_2O_4, and $KSm(PO_3)_4$ in glasses containing Sm_2O_3 or Dy_2O_3. In particular, it has been proposed that crystals of $Sm_xBi_{1-x}BO_3$ and β-BaB_2O_4 in the lines might be single crystals.[15–17] This technique is called *samarium (rare-earth) atom heat processing.*[15,16] In the samarium atom heat processing, cw Nd:YAG laser with $\lambda=1064$ nm is absorbed by Sm^{3+} in glass through f-f transitions ($^6F_{9/2} \leftarrow {}^6H_{5/2}$) and the surrounding of Sm^{3+} is heated through a nonradiative relaxation (electron-phonon coupling).[10–18] Consequently, structural modification (refractive index change) or crystallization is induced. It is of interest to apply the samarium atom heat processing to various glass-forming systems and to write crystal dots and lines showing nonlinear optical and ferroelectric properties, because crystals patterned at micrometer and nanoscales in glass substrates have a high potential for photonic devices. It should be emphasized that Nd:YAG laser is a conventional laser compared with other kinds of lasers such as short-wavelength excimer laser or femtosecond pulsed laser.

In this study, we try to write crystal lines consisting of $Sm_2(MoO_4)_3$ ferroelectrics in glasses based on the system Sm_2O_3–MoO_3–B_2O_3 by samarium atom heat processing. Rare-earth molybdates, $RE_2(MoO_4)_3$, (RE: trivalent rare-earth ions) are well-known crystals possessing various interesting ferroelectric, ferroelastic, and nonlinear optical properties.[19–27] For instance, they exhibit a comparatively large electro-optic effect and have potential applications in electro-optical devices. It has been reported that $Sm_2(MoO_4)_3$ crystal has a ferroelectric phase-transition (Curie) temperature of $T_C=197$ °C.[28] Since there has been no report on the crystallization of $Sm_2(MoO_4)_3$ in glasses, we have also developed Sm_2O_3–MoO_3–B_2O_3 glasses giving the formation of $Sm_2(MoO_4)_3$ by crystallization in this study.

[a)]Author to whom correspondence should be addressed; electronic mail: komatsu@chem.nagaokaut.ac.jp

II. EXPERIMENT

Commercial powders of reagent grade Sm_2O_3, MoO_3, and B_2O_3 were melted in a platinum crucible at 1000 °C for 30 min in an electric furnace. A small amount of CeO_2 (0.1 mol %) was added to reduce the dark brown color of $Sm_2O_3-MoO_3-B_2O_3$ glasses. The melts were poured onto an iron plate and pressed to a thickness of about 1–1.5 mm by another iron plate. The glass transition, T_g, and crystallization peak, T_p, temperatures were determined using differential thermal analysis (DTA) at a heating rate of 10 K/min. The quenched glasses were annealed at $\sim T_g$ to release internal stress and then polished mechanically to a mirror finish with CeO_2 powders.

Glasses were heat treated at T_p, and the crystalline phases present in the crystallized samples were identified by x-ray diffraction (XRD) analyses (Cu $K\alpha$ radiation) at room temperature. Micro-Raman-scattering spectra at room temperature for the precursor glasses and crystallized samples were measured with a laser microscope (Tokyo Instruments Co., Nanofinder) operated at Ar^+ (488 nm) laser. In our micro-Raman apparatus, the data below $\sim 300\ cm^{-1}$ cannot be measured due to the use of edge filter. Curie temperatures of crystallized samples were examined by using a differential scanning calorimetry (DSC) (Rigaku, DSC 8230D). Second-harmonic (SH) intensities of crystallized powders at room temperature were evaluated using the powder method proposed by Kurtz and Perry.[29] A fundamental wave of a *Q*-switched Nd:YAG laser operating at a wavelength of $\lambda = 1064$ nm was used as the incident light. The SH intensity of α-quartz powders was used as a reference.

A cw Nd:YAG laser operating at 1064 nm irradiated the polished surface of the glasses with a mirror finish. The laser beam was focused at the surface of the glasses using an objective lens ($20\times$, NA=0.4). By using a three-dimensional translation stage, focused positions of laser beam were moved at a constant speed. The laser powers were 0.4 W, and translation speeds of the sample stage were 1, 10, and 25 μm/s. The lines written by YAG laser irradiation were observed with a polarization optical microscope. Second-harmonic generation (SHG) emissions ($\lambda = 532$ nm) from crystal lines were measured with SHG microscopy.[30]

III. RESULTS AND DISCUSSION

A. Structural features of $Sm_2(MoO_4)_3$ crystals

The phase diagram and structure of rare-earth molybdates, $RE_2(MoO_4)_3$, where RE=Pr, Nd, Sm, Eu, Gd, Tb, Dy, have been studied extensively, and it is known that they show various structural types and a temperature-dependent polymorphism.[31–34] The thermodynamically stable phase in the temperatures below 800–990 °C is the α phase with a monoclinic structure ($C2/c$). In the temperature range of $1000 < T < 1200$ °C, the β phase with a tetragonal structure ($P42_1m$) is stable. The β phase (paraelectric) transforms to the β' phase (ferroelectric) with an orthorhombic structure ($Pba2$) below the Curie temperature.[34] The Curie temperature of the ferroelectric β'-phase $Sm_2(MoO_4)_3$ is reported to be $T_C = 197$ °C.[28] According to Nassau *et al.*,[32] the transformation from the α phase to the β phase occurs easily (fast), but the phase transition from the β phase to the α phase is slow kinetically. The structure of the orthorhombic $RE_2(MoO_4)_3$ phase is formed by REO_7 polyhedra (monocapped trigonal prisms) and MoO_4 tetrahedra, which are linked together via common corners.[35] Bonneville and Auzel[21] measured linear and nonlinear (second-order) susceptibilities of several $RE_2(MoO_4)_3$ crystals and proposed that the major part of nonlinear optical properties is due to the orientation of MoO_4 tetrahedra and the Mo–O bond hyperpolarizability.

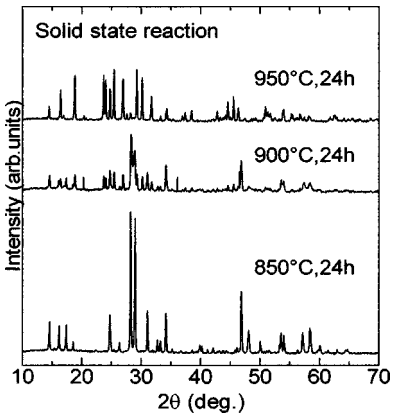

FIG. 1. XRD patterns at room temperature for the samples ($25Sm_2O_3 . 75MoO_3$) prepared by solid-state reaction.

Considering the structural features of $RE_2(MoO_4)_3$ crystals, it is of importance to distinguish the β'-$Sm_2(MoO_4)_3$ phase from the α-$Sm_2(MoO_4)_3$ phase in the present study. Prior to the crystallization of $Sm_2O_3-MoO_3-B_2O_3$ glasses, therefore, both of the α- and β'-$Sm_2(MoO_4)_3$ phases were prepared by a solid-state reaction (powder sintering method) with a help of the phase diagram of the system $Sm_2O_3-MoO_3$ reported by Nassau *et al.*,[32] and XRD patterns and Raman-scattering spectra for these phases were obtained. Since the data on XRD patterns and Raman-scattering spectra for $Sm_2(MoO_4)_3$ crystals are scarce and insufficient, we compared our data with the data for $Gd_2(MoO_4)_3$ crystals which have been extensively studied so far by many researchers.[31–37] The α-$Sm_2(MoO_4)_3$ phase was obtained by a sintering at 850 °C for 24 h, designated here as sample 1, and the β'-$Sm_2(MoO_4)_3$ phase was prepared by a sintering at 950 °C for 24 h, designated here as sample 2. The XRD patterns for these samples are shown in Fig. 1. It was confirmed that the XRD pattern for sample 2 is the same as that (JCPDS: No. 20-408) for the β'-$Gd_2(MoO_4)_3$ phase. We heat treated again sample 2 at 850 °C for 40 h and confirmed that the XRD pattern for this sample is the same as that for sample 1. This result indicates that the phase transformation between the β'-$Sm_2(MoO_4)_3$ phase and the α-$Sm_2(MoO_4)_3$ phase occurs, supporting the phase diagram reported by Nassau *et al.*[32]

The Raman-scattering spectra for the sintered samples are shown in Fig. 2, where sample 1 gives the peaks at 396, 783, and 902 cm^{-1} and sample 2 shows the peaks at 326, 384, 744, 815, 848, 943, and 957 cm^{-1}. It was confirmed that the Raman spectrum for sample 2 is almost the same as that for the β'-$Gd_2(MoO_4)_3$ phase showing the peaks at 321, 362,

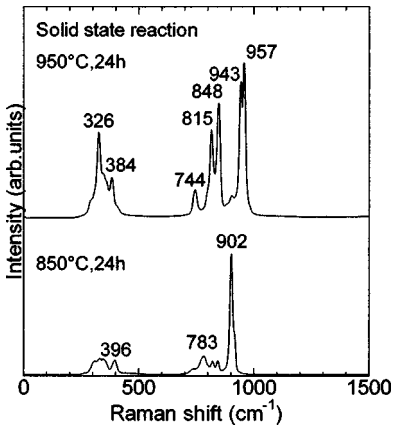

FIG. 2. Raman-scattering spectra at room temperature for the samples ($25Sm_2O_3.75MoO_3$) prepared by solid-state reaction.

750, 857, 943, and 960 cm^{-1}.[35] The DSC patterns for the sintered samples were measured, and a clear endothermic peak was observed at around 198 °C for sample 2. As reported by Roy *et al.*,[28] this endothermic peak is assigned to the phase transition from the ferroelectric state (β' phase) to the paraelectric state (β phase) in $Sm_2(MoO_4)_3$ crystals with $T_C=197$ °C. On the other hand, no endothermic peak was detected at temperatures around 195 °C for sample 1. These results shown in Figs. 1 and 2 demonstrate that the crystalline phases formed in sample 1 (sintered at 850 °C for 24 h) and sample 2 (sintered at 950 °C for 24 h) are the α -$Sm_2(MoO_4)_3$ phase and the β'-$Sm_2(MoO_4)_3$ phase, respectively. The XRD patterns and Raman-scattering spectra for the α- and β'-$Sm_2(MoO_4)_3$ phases obtained in the present study are used for the identification of crystalline phases formed in crystallized glasses and crystal lines written by YAG laser irradiation.

B. Glass formation in the Sm_2O_3–MoO_3–B_2O_3 system

In the samarium atom heat processing, it is a key point to find glasses containing some amounts of Sm_2O_3 and giving the formation of target crystals by crystallization. Since a sample with the chemical composition of $Sm_2(MoO_4)_3$ does not form any glassy form in a conventional melt quenching method, we need to develop glasses containing both Sm_2O_3 and MoO_3. Considering previous studies,[10–18] it is desired to develop glasses with Sm_2O_3 contents of 8–15 mol % for the application of samarium atom heat processing. It is known that borate glasses generally provide large solubility of rare-earth oxides, and this is the reason why we chose system of Sm_2O_3–MoO_3–B_2O_3 in this study. The glass-forming region in the system of Sm_2O_3–MoO_3–B_2O_3, however, has not been reported so far. Since the purpose of this study is to develop crystallized glasses consisting of the β' -$Sm_2(MoO_4)_3$ phase, i.e., $MoO_3/Sm_2O_3=3$, we examined the glass formation for various compositions with the Sm_2O_3/MoO_3 ratio of around three and with small amounts of B_2O_3. Consequently, although the glass-forming ability in the system of Sm_2O_3–MoO_3–B_2O_3 was found to be poor, we succeeded in developing some glasses such as $20Sm_2O_3.50MoO_3.30B_2O_3$ and $20Sm_2O_3.60MoO_3.20B_2O_3$. In this study, we use the glass of $21.25Sm_2O_3.63.75MoO_3.15B_2O_3$ (designated here as SMB glass), because the β'-$Sm_2(MoO_4)_3$ phase is formed by crystallization, as will be described in Sec. III C. The DTA pattern for SMB glass is shown in Fig. 3. An endothermic peak due to the glass transition and an exothermic peak due to the crystallization are observed, giving the values of $T_g=528$ °C and $T_p=572$ °C. The difference between T_p and T_g is small, i.e., $\Delta T=T_p-T_g=44$ °C, suggesting that the thermal stability against crystallization in SMB glass is not so high and crystallization would occur easily.

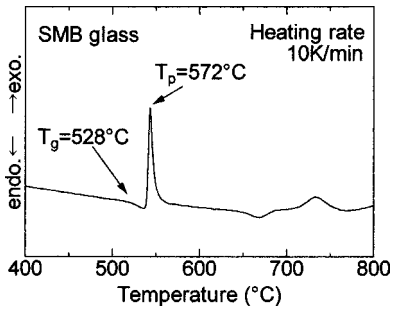

FIG. 3. DTA pattern for $21.25Sm_2O_3.63.75MoO_3.15B_2O_3$ glass. Heating rate was 10 K/min.

Recently, Das and Ambika[38] examined the local structure of $80MoO_3.20B_2O_3$ glass ($T_g=350$ °C) using electron paramagnetic resonance and infrared spectra and reported that the ratio of $Mo^{6+}/(Mo^{6+}+Mo^{5+})$ is 0.67 and molybdenum ion is in a distorted octahedral environment of six oxygen atoms. Their study proposes that MoO_3 oxide in their glass acts as glass former. In our SMB glass, the main component is MoO_3 and its amount is 63.75 mol %. Although the structure of Sm_2O_3–MoO_3–B_2O_3 glasses has not been studied, it is considered that MoO_3 in our SMB glass would also act as glass former. The glass-forming region, properties, and structure of binary rare-earth borate glasses have been studied extensively so far. For instance, in the Sm_2O_3–B_2O_3 system, glasses can be formed in the range from 0 to ~30 mol % Sm_2O_3, but the liquid immiscibility limits the range of homogeneous glasses to 0–1.5 and 20–30 mol % Sm_2O_3.[39,40] Indeed, even in the system Sm_2O_3–MoO_3–B_2O_3, it was found that the melt-quenched samples containing 10 mol % Sm_2O_3 consisted of two phases: the crystalline part at the surface and the glassy part in the interior, implying the presence of liquid immiscibility. In this study, we succeeded in developing Sm_2O_3–MoO_3–B_2O_3 glasses containing ~20 mol % Sm_2O_3. It should be pointed out that the Sm_2O_3 content giving the glass formation in the ternary Sm_2O_3–MoO_3–B_2O_3 system is similar to that in the binary Sm_2O_3–B_2O_3 system, even though B_2O_3 contents in both systems are largely different. The structure of Sm_2O_3–MoO_3–B_2O_3 glasses will be again discussed in Sec. III C.

C. Formation of ferroelectric β'-$Sm_2(MoO_4)_3$ in crystallized glasses

The XRD pattern and Raman-scattering spectrum for the SMB crystallized sample obtained by heat treatment at

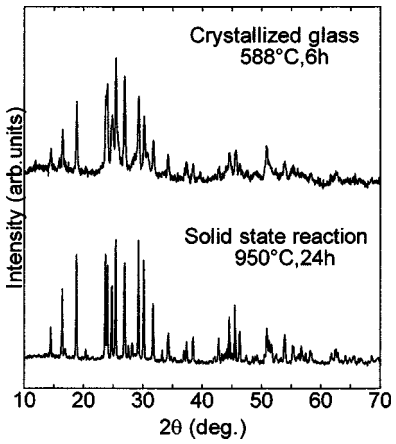

FIG. 4. XRD patterns at room temperature for the sample ($25Sm_2O_3.75MoO_3$) prepared by solid-state reaction and for the crystallized glass ($21.25Sm_2O_3.63.75MoO_3.15B_2O_3$).

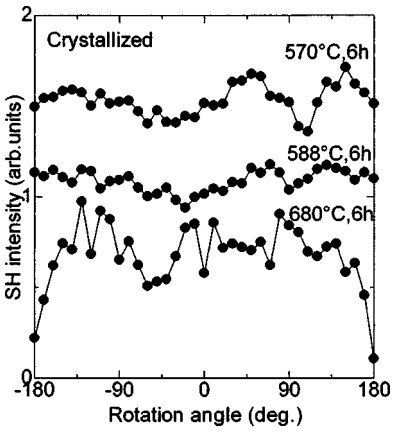

FIG. 6. Second-harmonic intensities obtained by using Kurtz and Perry's powder method for crystallized powder samples of $21.25Sm_2O_3.63.75MoO_3.15B_2O_3$.

588 °C for 6 h are shown in Figs. 4 and 5, respectively. The data of the XRD and Raman spectrum indicate clearly the formation of the β'-$Sm_2(MoO_4)_3$ phase in the SMB crystallized sample. The Raman-scattering spectrum for the SMB crystallized sample heat treated at 719 °C for 6 h is shown in Fig. 5. The appearance of the strong peak at 900 cm^{-1} indicates the formation of the α-$Sm_2(MoO_4)_3$ phase besides the β'-$Sm_2(MoO_4)_3$ phase, suggesting the start of the transformation of the β'-$Sm_2(MoO_4)_3$ phase to the α-$Sm_2(MoO_4)_3$ phase. The SH intensities for the SMB crystallized samples obtained by heat treatments at 570, 588, and 680 °C for 6 h are shown in Fig. 6. In these experiments, the powdered samples (shaped to disk plate) were rotated against incident measuring YAG laser to minimize the data scattering of SH intensity due to the inhomogeneous packing of powders. The strong SHGs are clearly observed in all samples. Furthermore, it should be pointed out that the SH intensity depends on the heat-treatment temperature, i.e., the SH intensity of the crystallized sample heat treated at 570 °C is stronger than those of the samples heat treated at 588 and 680 °C. These results demonstrate that the ferroelectric β'-$Sm_2(MoO_4)_3$ phase showing a second-order optical nonlinearity is primarily precipitated and then the paraelectric α-$Sm_2(MoO_4)_3$ phase is formed in the crystallization of SMB glass, as already suggested from the Raman-scattering spectra (Fig. 5). In the phase diagram of the system Sm_2O_3–MoO_3 reported by Nassau *et al.*,[32] the low-temperature phase below ~880 °C is the α-$Sm_2(MoO_4)_3$ phase and the high-temperature phase above ~880 °C is the β-$Sm_2(MoO_4)_3$ phase. In the crystallization of SMB glass, however, the β-$Sm_2(MoO_4)_3$ phase is directly appeared by relatively low-temperature heat treatment prior to the formation of the α-$Sm_2(MoO_4)_3$ phase. Since the heat-treatment temperature of ~600 °C for the crystallization of SMB glass corresponds to the temperature being stable for the α-$Sm_2(MoO_4)_3$ phase, it is considered that the β-$Sm_2(MoO_4)_3$ phase formed initially through the crystallization is not stable thermodynamically and thus tends to transform to the α-$Sm_2(MoO_4)_3$ phase during heat treatment at ~600 °C. Anyway, the fact that the primary crystalline phase in SMB glass is the β-$Sm_2(MoO_4)_3$ phase indicates that SMB glass is a good precursor glass in the present study.

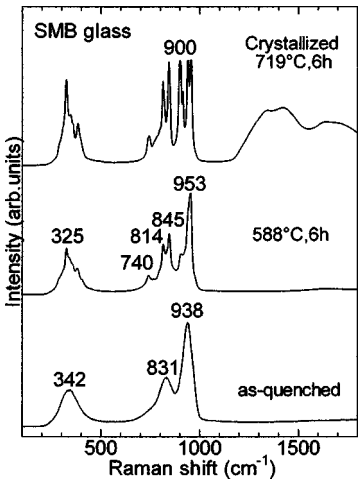

FIG. 5. Raman-scattering spectra at room temperature for the glass and crystallized samples of $21.25Sm_2O_3.63.75MoO_3.15B_2O_3$.

The Raman-scattering spectrum for the precursor SMB glass is shown in Fig. 5. Although the peaks are broad, being typical for glass materials, the peak positions are very similar to those for the β'-$Sm_2(MoO_4)_3$ phase, but not similar to those for the α-$Sm_2(MoO_4)_3$ phase. In the structure of the β'-$RE_2(MoO_4)_3$ phase, MoO_4 tetrahedra and REO_7 polyhedra are linked together via common corners.[35] The Raman-scattering spectra shown in Fig. 5 strongly suggest the structural similarity between the precursor glass and the β'-$Sm_2(MoO_4)_3$ phase, and this would be one of the reasons for the primarily crystallization of the β'-$Sm_2(MoO_4)_3$ phase in SMB glass. The coordination state of Mo^{6+} ions in some glasses such as MoO_3–TeO_2 has been examined from Raman-scattering and infrared spectra.[38,41–44] It has been reported that MoO_4 tetrahedra and MoO_6 octahedra are present as basic structural units. Neov *et al.*[41] reported that an increase in MoO_3 content results in a sequential conversion of Mo^{6+} from MoO_6 to MoO_4. The structural unit of MoO_4 tetrahedron gives the band at 840–850 cm^{-1} in Raman-scattering and infrared spectra.[42,44] The broad peak at

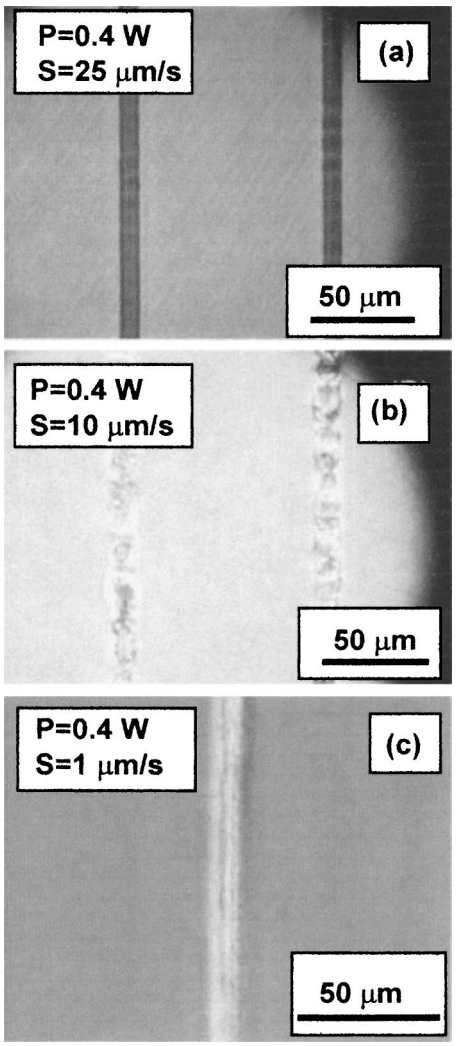

FIG. 7. Polarization optical microphotographs (top views) for the samples obtained by cw Nd:YAG laser irradiations with a laser power of $P=0.4$ W and sample moving speeds of $S=1$, 10, and 25 μm/s. The glass is $21.25Sm_2O_3.63.75MoO_3.15B_2O_3$.

820 cm^{-1} in Fig. 5 would support the presence of MoO_4 tetrahedral units in SMB glass containing of a large amount (63.75 mol %) of MoO_3.

D. Writing of nonlinear optical β'-$Sm_2(MoO_4)_3$ crystal lines by YAG laser irradiation

As stated above, we developed glasses in the system $Sm_2O_3-MoO_3-B_2O_3$, which give the formation of nonlinear optical β'-$Sm_2(MoO_4)_3$ crystals through conventional crystallization in an electric furnace. We tried to write β'-$Sm_2(MoO_4)_3$ crystal lines at the surface of SMB glass by irradiation of cw Nd:YAG laser, i.e., the samarium atom heat processing. The polarization optical microphotographs for the samples obtained by YAG laser irradiation are shown in Fig. 7, where the laser power was $P=0.4$ W and the moving speeds of the glass were $S=1$, 10, and 25 μm/s. It is seen that structural changes are induced by YAG laser irradiation and their morphologies depend on laser scanning speed. The micro-Raman-scattering spectrum for the line [(a) in Fig. 7] written with $S=25$ μm/s is shown in Fig. 8, where those of the precursor glass and β'-$Sm_2(MoO_4)_3$ crystals (sample 2)

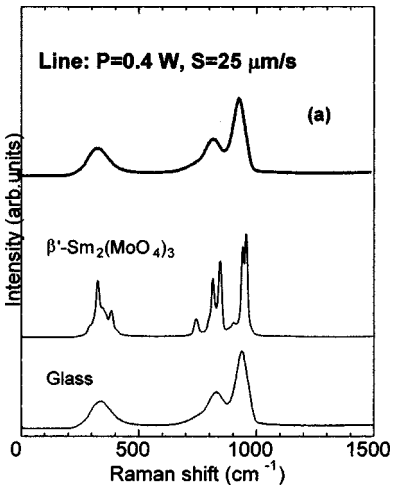

FIG. 8. Micro-Raman scattering spectrum (a) at room temperature for the line written by YAG laser irradiation with a power of 0.4 W and a scanning speed of 25 μm/s in $21.25Sm_2O_3.63.75MoO_3.15B_2O_3$ glass. The spectra for the precursor glass and β'-$Sm_2(MoO_4)_3$ crystals prepared by a solid-state reaction are included for comparison.

prepared by a solid-state reaction (950 °C, 24 h) are included for comparison. Since the spectrum for the line is almost the same as that for the precursor glass, it is concluded that the line does not consist of crystals but is still amorphous. That is, the YAG laser irradiation with a high moving speed of $S=25$ μm/s induces only refractive index changes. It is considered that the temperature of the laser-irradiated region would be heated to temperatures around the glass transition temperature ($T_g=528$) and structural modifications (not crystallization, but just density fluctuations) are induced.

The micro-Raman-scattering spectrum for the line [(b) in Fig. 7] written with $S=10$ μm/s is shown in Fig. 9, demonstrating that the line consists of β'-$Sm_2(MoO_4)_3$ crystals. Since SMB glass has the values of $T_g=528$ and $T_p=572$ °C, it is considered that the temperature of the laser-

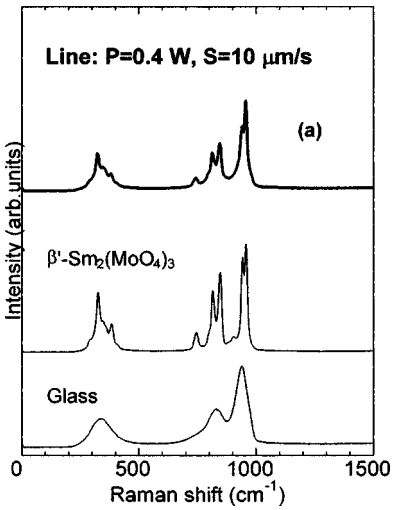

FIG. 9. Micro-Raman-scattering spectrum (a) at room temperature for the line written by YAG laser irradiation with a power of 0.4 W and a scanning speed of 10 μm/s in $21.25Sm_2O_3.63.75MoO_3.15B_2O_3$ glass. The spectra for the precursor glass and β'-$Sm_2(MoO_4)_3$ crystals prepared by a solid-state reaction are included for comparison.

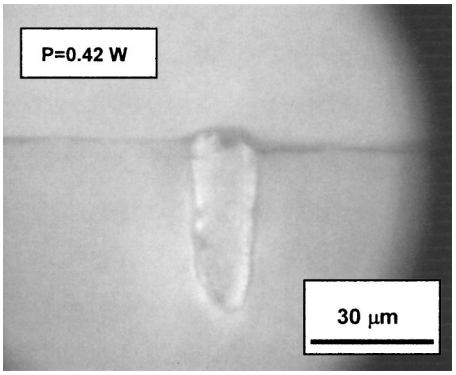

FIG. 10. Polarization optical microphotograph for the cross section of a crystal line written by YAG laser irradiation ($P=0.42$ W, $S=10$ μm/s) in $21.25Sm_2O_3.63.75MoO_3.15B_2O_3$ glass.

irradiated region would be at least above 530 °C. As seen in Fig. 7, the growth of β'-$Sm_2(MoO_4)_3$ crystals is not smooth, but seems to be discontinuous. The SHG microscope measurements were performed for the lines consisting of β'-$Sm_2(MoO_4)_3$ crystals, and SHGs were clearly observed from the lines, demonstrating that $Sm_2(MoO_4)_3$ crystals in the lines are nonlinear optical crystals as similar to the case in the crystallized glasses obtained by heat treatment in an electric furnace.

As seen in Fig. 7, a line written with $S=1$ μm/s shows a relatively homogeneous color in a polarization optical microphotograph compared with the line written with $S=10$ μm/s. The SHGs were clearly observed in the crystal lines written with 1 μm/s. It was confirmed from the micro-Raman-scattering spectra that these lines consist of β'-$Sm_2(MoO_4)_3$ crystals, although the spectra suggest the formation of the α-$Sm_2(MoO_4)_3$ phase also. Very slow writing speeds might induce the transformation of the β'-$Sm_2(MoO_4)_3$ phase to the α-$Sm_2(MoO_4)_3$ phase during laser irradiation. It is considered that the optimum scanning condition for the writing of homogeneous crystal lines consisting of only the β'-$Sm_2(MoO_4)_3$ phase would be present in the range of 1–10 μm/s, when the YAG laser power is fixed to 0.4 W.

In the samarium atom heat processing, cw Nd:YAG laser with $\lambda=1064$ nm is absorbed by Sm^{3+} in glass through *f-f* transitions ($^6F_{9/2} \leftarrow {}^6H_{5/2}$) and the surrounding of Sm^{3+} is heated through a nonradiative relaxation (electron-phonon coupling).[10–18] Consequently, structural modification (refractive index change) or crystallization is induced. When we used a nanopulse Nd:YAG laser with $\lambda=1064$ nm instead of cw Nd:YAG laser, no crystallization was induced in the Sm_2O_3–MoO_3–B_2O_3 glasses. This means that it is necessary to irradiate laser continuously to keep high temperatures (greater than crystallization temperature) and to induce crystallization in the laser-irradiated region. In other words, the heat dissipation from the laser-irradiated region to the surrounding glass medium occurs rapidly. Considering the heat balance between the laser energy absorbed by Sm^{3+} and heat dissipation, the temperature of the cw Nd:YAG laser-irradiated region in glass would depend on the amount of Sm^{3+} in glass, laser power, laser scanning speed, specific heat, and thermal conductivity of glass. Furthermore,

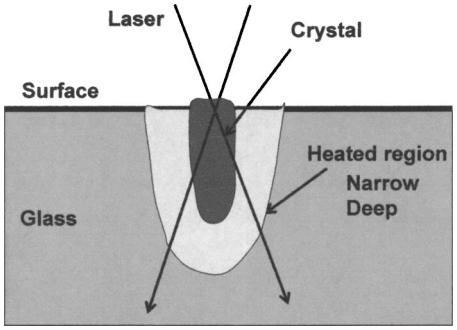

FIG. 11. A schematic illustration of the model for the crystal growth at the YAG laser-irradiated region.

whether crystallization by YAG laser irradiation occurs or not will depend not only on the temperature of laser-irradiated region but also on the thermal stability against crystallization. Indeed, the formation of crystal lines by YAG laser irradiation has been observed in glasses containing some amounts of Sm_2O_3 contents such as 10 mol % and in glasses having the strong tendency of the crystallization,[10–18] as in $21.25Sm_2O_3.63.75MoO_3.15B_2O_3$ glass developed in this study.

The polarization optical microphotograph for the cross section of a crystal line written by YAG laser irradiation ($P=0.42$ W, $S=10$ μm/s) in SMB glass is shown in Fig. 10. It was confirmed from the micro-Raman-scattering spectra that this consists of β'-$Sm_2(MoO_4)_3$ crystals, indicating that β'-$Sm_2(MoO_4)_3$ crystals grow deeply into the interior of the glass during laser scanning. Furthermore, a swelling at the surface is observed, suggesting the formation of a melt in the laser-irradiated region. Considering the shape of crystals in the interior of the glass shown in Fig. 10, we propose that the region with high temperatures being sufficient for the crystallization would be narrow and also deep. The model is shown in Fig. 11 schematically. One of the reasons for such a temperature distribution would be due to the use of the lens with a small numerical aperture of NA=0.4 in this study. A preliminary computer simulation on the temperature at the laser-irradiated region supports the corn-shape temperature distribution.[45]

IV. CONCLUSION

Some glasses such as $21.25Sm_2O_3.63.75MoO_3.15B_2O_3$ (mol %) giving the formation of nonlinear optical $Sm_2(MoO_4)_3$ crystals through conventional crystallization in an electric furnace and through continuous-wave Nd:YAG laser (wavelength: 1064 nm) irradiation (*samarium atom heat processing*) were developed. It was found from x-ray diffraction analyses, micro-Raman-scattering spectra, and second-harmonic generation measurements that the crystal structure of $Sm_2(MoO_4)_3$ formed by the crystallization is the β'-phase structure with an orthorhombic (noncentrosymmetric) symmetry. The lines consisting of β'-$Sm_2(MoO_4)_3$ crystals were written at the surface of glasses by YAG laser irradiation (laser power: $P=0.4$ W, laser scanning speed: $S=1-10$ μm/s), and, in particular, at the laser scanning speed of 1 μm/s relatively homogeneous crystal lines were formed. The refractive index changes (not crystallization)

were also induced by YAG laser irradiation of $P=0.4$ W and a high laser scanning speed of $S=25\ \mu$m/s. The present study demonstrates that the samarium atom heat processing is a technique for the writing of rare earth containing optical nonlinear/ferroelectric crystal lines in glass.

ACKNOWLEDGMENTS

This work was supported from Ministry of Internal Affairs and Communications Strategic Information and Communications R&D Promotion Programs (SCOPE), Grant-in-Aid for Scientific Research from the Ministry of Education, Science, Sports, Culture and Technology, Japan, and by the 21st Century Center of Excellence (COE) Program in Nagaoka University of Technology.

[1]G. H. Beall and D. A. Duke, J. Mater. Sci. **4**, 340 (1969).
[2]K. Shioya, T. Komatsu, H. G. Kim, R. Sato, and K. Matusita, J. Non-Cryst. Solids **189**, 16 (1995).
[3]F. Torres, K. Narita, Y. Benino, T. Fujiwara, and T. Komatsu, J. Appl. Phys. **94**, 5265 (2003).
[4]Y. Takahashi, Y. Benino, T. Fujiwara, and T. Komatsu, J. Appl. Phys. **95**, 3503 (2004).
[5]D. Du, X. Liu, G. Korn, J. Squier, and G. Mourou, Appl. Phys. Lett. **64**, 3071 (1994).
[6]K. M. Davis, K. Miura, N. Sugimoto, and K. Hirao, Opt. Lett. **21**, 1729 (1996).
[7]T. Fujiwara, R. Ogawa, Y. Takahashi, Y. Benino, T. Komatsu, and J. Nishii, Phys. Chem. Glasses **43C**, 213 (2002).
[8]C. B. Schaffer, A. O. Jamison, and E. Mazur, Appl. Phys. Lett. **84**, 1441 (2004).
[9]H. Ebendorff-Heidepriem, Opt. Mater. **25**, 109 (2004).
[10]R. Sato, Y. Benino, T. Fujiwara, and T. Komatsu, J. Non-Cryst. Solids **289**, 228 (2001).
[11]T. Honma, Y. Benino, T. Fujiwara, R. Sato, and T. Komatsu, Opt. Mater. **20**, 27 (2002).
[12]T. Honma, Y. Benino, T. Fujiwara, R. Sato, and T. Komatsu, J. Ceram. Soc. Jpn. **110**, 398 (2002).
[13]S. Kawasaki, T. Honma, Y. Benino, T. Fujiwara, R. Sato, and T. Komatsu, J. Non-Cryst. Solids **325**, 61 (2003).
[14]H. Tanaka, T. Honma, Y. Benino, T. Fujiwara, and T. Komatsu, J. Phys. Chem. Solids **64**, 1179 (2003).
[15]T. Honma, Y. Benino, T. Fujiwara, T. Komatsu, and R. Sato, Appl. Phys. Lett. **82**, 892 (2003).
[16]T. Honma, Y. Benino, T. Fujiwara, T. Komatsu, and R. Sato, Appl. Phys. Lett. **83**, 2796 (2003).
[17]T. Honma, Y. Benino, T. Fujiwara, R. Sato, and T. Komatsu, J. Phys. Chem. Solids **65**, 1705 (2004).
[18]M. Saito, T. Honma, Y. Benino, T. Fujiwara, and T. Komatsu, Solid State Sci. **6**, 1013 (2004).
[19]H. J. Borchardt and P. E. Bierstedt, Appl. Phys. Lett. **8**, 50 (1966).
[20]A. Kumada, Ferroelectrics **3**, 115 (1972).
[21]R. Bonneville and F. Auzel, J. Chem. Phys. **67**, 4597 (1977).
[22]A. A. Berezhnoi, Opt. Spectrosc. **77**, 548 (1994).
[23]B. K. Ponomarev, V. D. Negrii, B. S. Red'kin, and Y. F. Popov, J. Phys. D **27**, 1995 (1994).
[24]H. Nishioka, W. Odajima, M. Tateno, K. Ueda, A. A. Kaminskii, A. V. Butashin, S. N. Bagayev, and A. A. Pavlyuk, Appl. Phys. Lett. **70**, 1366 (1997).
[25]D. Xue and S. Zhang, J. Phys. Chem. Solids **59**, 1337 (1998).
[26]D. Jaque, Z. D. Luo, and J. G. Sole, Appl. Phys. B: Lasers Opt. **72**, 811 (2001).
[27]D. C. Lupascu, V. Y. Shur, and A. G. Shur, Appl. Phys. Lett. **80**, 2359 (2002).
[28]M. Roy, R. N. P. Choudhary, and H. N. Acharya, Thermochim. Acta **145**, 11 (1989).
[29]S. K. Kurtz and T. T. Perry, J. Appl. Phys. **39**, 3798 (1968).
[30]T. Fujiwara, T. Sawada, T. Honma, Y. Benino, T. Komatsu, M. Takahashi, T. Yoko, and J. Nishii, Jpn. J. Appl. Phys., Part 1 **42**, 7326 (2003).
[31]K. Nassau, H. J. Levinstein, and G. M. Loiacono, J. Phys. Chem. Solids **26**, 1805 (1965).
[32]K. Nassau, J. W. Shiever, and E. T. Keve, J. Solid State Chem. **3**, 411 (1971).
[33]W. Jeitschko, Acta Crystallogr., Sect. B: Struct. Crystallogr. Cryst. Chem. **28**, 60 (1972).
[34]V. Dimitriev, V. Sinitsyn, R. Dilanian, D. Machon, A. Kuznetsov, E. Ponyatovsky, G. Lucazeau, and H. P. Weber, J. Phys. Chem. Solids **64**, 307 (2003).
[35]A. A. Kaminskii *et al.*, Opt. Mater. **7**, 59 (1997).
[36]H. J. Borchardt and P. E. Bierstedt, J. Appl. Phys. **38**, 2057 (1967).
[37]L. H. Brixner, P. E. Bierstedt, A. W. Sleight, and M. S. Licis, Mater. Res. Bull. **6**, 545 (1971).
[38]B. B. Das and R. Ambika, Chem. Phys. Lett. **370**, 670 (2003).
[39]I. N. Chakraborty, D. E. Day, J. C. Lapp, and J. E. Shelby, J. Am. Ceram. Soc. **68**, 368 (1985).
[40]K. Terashima, S. Tamura, S. H. Kim, and T. Yoko, J. Am. Ceram. Soc. **80**, 2903 (1997).
[41]S. Neov, I. Gerasimova, B. Sidzhimov, V. Kozhukharov, and P. Mikula, J. Mater. Sci. **23**, 347 (1988).
[42]R. Iordanova, Y. Dimitriev, V. Dimitrov, and D. Klissurski, J. Non-Cryst. Solids **167**, 74 (1994).
[43]T. Sekiya, N. Mochida, and S. Ogawa, J. Non-Cryst. Solids **185**, 135 (1995).
[44]A. Mogus-Milankovic, A. Santic, A. Gajovic, and D. E. Day, J. Non-Cryst. Solids **325**, 76 (2003).
[45]Y. Benino, T. Fujiwara, and T. Komatsu (unpublished).